THE PERFORMANCE CHARACTERISTICS OF COMPLIANT SHELL LEMON BORE BEARINGS

S. C. JAIN, M. MALIK and R. SINHASAN

Department of Mechanical and Industrial Engineering
University of Roorkee
Roorkee 247 667, India
Received October 27, 1987
Presented by Prof. Dr. L. Varga

Abstract

Lemon-bore bearings are quite popular in high speed applications. In this paper the effects of bearing deformation on the performance characteristics of lemon shaped journal bearing systems are determined. Modifying the extent of film in each lobe with shell deformation, the results are calculated for wide range of operating eccentricity and different values of ellipticity ratio and deformation coefficient. This study reveals many favourable changes in performance characteristics of the journal bearing system if supported on flexible bearings.

Nomenclature:

The symbols with a bar represent dimensional quantities.

$\bar{B}$	bearing length
$\bar{C}, C_m$	clearances defined in Fig. 1
$\bar{E}$	Young's modulus of bearing liner
H_L	film thickness, $\bar{H}_L/\bar{C}_m$
L	subscript or superscript for lobe, $=1, 2$
M_c	critical mass of journal, $\bar{M}_c/((\bar{\mu}_0\bar{R}_j/\bar{\omega}_j)(\bar{R}_j/\bar{C}_m)^3)$
p	pressure, $\bar{p}/((\bar{\mu}_0\bar{\omega}_j)(\bar{R}_j/\bar{C}_m)^2)$
$p_{\max}$	maximum pressure
T_j	viscous frictional torque on the journal, $\bar{T}_j/((\bar{\mu}_0\bar{\omega}_j\bar{R}_j^3)(\bar{R}_j/\bar{C}_m))$
Q_s	oil flow through sides, $\bar{Q}_s/(\bar{C}_m\bar{R}_j\bar{B}\bar{\omega}_j/2\pi)$
$\bar{R}_j$	journal radius
t	time, $\bar{t}\bar{\omega}_j$
t_h	bearing liner thickness, $\bar{t}_h/\bar{R}_j$
W_r	bearing load capacity, $\bar{W}_r/(\bar{\mu}_0\bar{\omega}_j\bar{R}_j^2/(\bar{R}_j/\bar{C}_m)^2)=W_y^2-W_y^1$
W_v^L	load component in vertical direction due to Lth lobe

x, y	coordinate axes defined in Fig. 1
X_J, Y_J	journal center coordinates, $(\bar{X}_J, \bar{Y}_J)/\bar{C}_m$
X_L, Y_L	lobe center coordinates in undeformed state of liner $(\bar{X}_L, \bar{Y}_L)/\bar{C}_m$
z	coordinate along bearing axis, $\bar{z}/\bar{R}_j$
δ_r	radial deformation, $\bar{\delta}_r/\bar{C}_m$
$\emptyset$	altitude angle, Fig. 1
λ	aspect ratio, $\bar{B}/(2\bar{R}_j)$
ε	eccentricity ratio, $\bar{\varepsilon}/\bar{C}_m$
ε_p	ellipticity ratio, $\bar{\varepsilon}_p/\bar{C}_m$
ν	Poisson's ratio
ν_0	$(1+\nu)(1-2\nu)/(1-\nu)$, Eq. [2]
$\bar{\mu}_0$	viscosity of lubricant
ψ	deformation coefficient, ψ_r/ν_0
$\psi_r, \psi_r^1=\delta_r/p,$	coefficients defined in Eqs. [1] and [2]
r, θ, z	cylindrical coordinates
$\{\delta\}$	nodal displacement vector, $\{\delta_\theta \delta_r \delta_z\}$

1. Introduction

The interest in elastohydrodynamic analysis of sliding bearings has grown only during the past two decades. Many investigations have now evidenced that the response of any rotating system supported on self-acting hydrodynamic bearings can not be predicted accurately, if design calculations are made by disregarding the deformation in the bearings. A noteworthy experimental study which successfully demonstrated the need of including deformation in plane journal bearings was due to Carl [1]. This pioneer study led to many theoretical and experimental investigations [2—8]. Amongst these, Higginson [2] presented in his famous paper a simplified formulation of ehd analysis of plane journal bearings. Relinquishing many assumptions of Higginson, O'Donghue et al, Conway and Lee, Oh and Heubaer, Jain et al and Gethin have carried out rigorous studies to investigate effects of deformation on the performance characteristics of plane journal bearings.

The work of this paper is concerned with ehd analysis of lemon-bore bearings. The interest in the study has arisen for the reason that such bearings because of their very suitability, often operate under heavy loads and high speeds leading to considerably large hydrodynamic pressures. The ehd analysis of journal bearings is problematic due to the iterative nature of problem and computation of bearing deformation thorugh the solution or 3-dimensional elasticity equations. The analysis in this work is carried out using a simple elastic model in bearing liner. However, prior to

using this model, a detailed investigation on the basis of 3-dimensional ehd analysis is made to show the suitability of the model to the actual practical conditions.

The results presented in the paper are intended to investigate the effect of liner deformation in lemon-bore bearings. These include the static characteristics and stability margins of the bearings.

2. Analysis

The lobed bearing is considered as comprising a liner (flexible element), of usual bearing material (like babbit, bronze, etc.) securely bonded inside a housing (rigid element) of some harder material (steel or cast iron), Fig. 1. The deformation analysis of the bearing liner may be treated as a linear three dimensional elasticity problem of a shell subject to a hydrodynamic pressure field. As a consequence of minimum potential energy theorem, the displacement field of the linear may be expressed by the

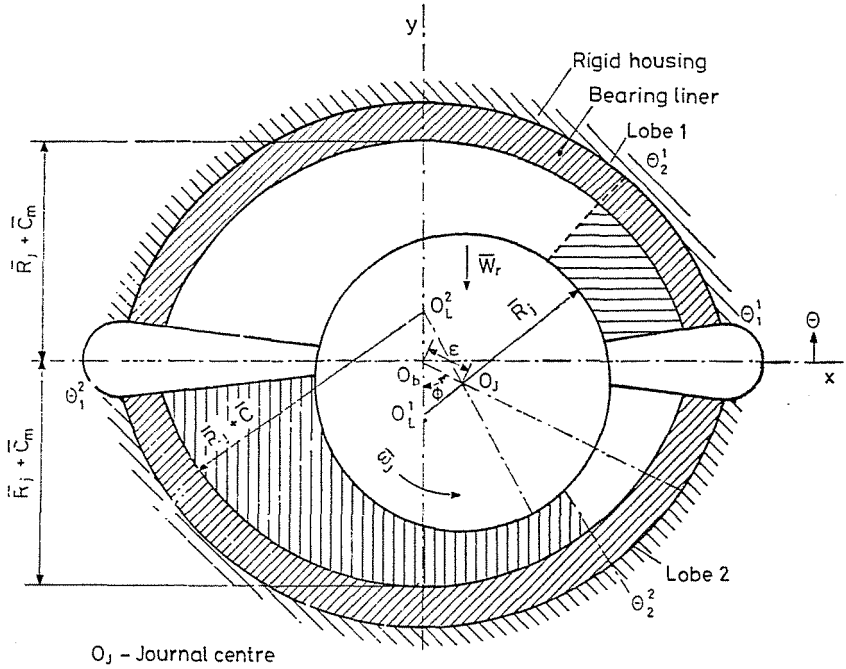

Fig. 1. Symmetrical two lobe bearing geometry with bearing liner

following set of finite element equations

$$[K]\{\delta\} = \{F\} \tag{1}$$

where $[K]$ is the stiffness matrix, $\{\delta\}$ is the vector of nodal displacements, and $\{F\}$ is the vector of nodal tractions due to external forces (pressure in the present case).

The present ehd analysis is in reality a coupled problem requiring simultaneous solution of the lubrication equation and the three dimensional elasticity equations. The analysis is however, computationally expensive due to very iterative nature of the problem. In fact, solution of elasticity equations needed in each iteration, takes up the major share of total computation time. In the ehd analysis of lobed bearing, the computation time increases nearly in proportion to the number of lobes. Therefore, for the ehd analysis of lobed bearings it becomes imperative to look for a simpler model of elastic field of bearing liner.

In the above regard, a simple model can be derived if the state of strain in bearing liner is assumed to be plain with axial strain (ε_z) equal to zero. This is taken on the basis that practical bearing liners are thin. With plain strain condition the radial deformation in a firmly bonded thin liner can be estimated with great accuracy by the linear relation

$$\delta_r(\theta, z) = \psi_r p(\theta, z) = \psi_0 p(\theta, z) \tag{2}$$

where

$$\psi_r = \left(\frac{\bar{\mu}_0 \bar{\omega}_j}{\bar{E}}\right)\left(\frac{\bar{t}_h}{\bar{R}_j}\right)\left(\frac{\bar{R}_j}{\bar{C}_m}\right)^3\left[\frac{(1+\nu)(1-2\nu)}{1-\nu}\right] \tag{3}$$

is a constant independent of the spatial coordinates (r, θ, z) and is written here as a combination of parameters representing the geometric and material properties of the liner and operating conditions of the bearing [6, 7].

As for the suitability of above model and finding the upper limit of liner thickness for the applicability of model, it would be interesting to look into Fig. 2 in which some results of 3-dimensional ehd analysis of 160° arc partial journal bearing are given. The case of partial bearing suits here as it is equivalent to a single lobe of a non-circular bearing. The operating conditions of bearing are taken as:

$$\bar{R}_j = 25 \text{ mm}, \quad \bar{B} = 50 \text{ mm}, \quad \bar{\mu}_0 = 0.04 \text{ Pas}, \quad \bar{C}_m/\bar{R}_j = 0.002$$

$$\bar{\omega}_j = 2500 \, rpm, \quad \bar{E} = 120 \text{ GPa}, \quad \nu = 0.3$$

with liner thicknesses $\bar{t}_h$ equal to 0 (rigid liner case), 2.5, 5 and 10 mm. In the figure, 2(a) and 2(b) show the circumferential distributions of radial deformation of liner ($\bar{\delta}_r$) at film interface, film thickness ($\bar{H}_L$) and pressure ($\bar{p}$), all three taken at bearing mid-span ($z=0$). Dividing the radial deformation at a point (from Fig. 2(a)) by pressure at the same point (from Fig. 2(b)) the ratio ψ_r' is obtained and is plotted in Fig. 2(c). This figure also include the variation of ψ_r' at quarter span ($z=\pm\lambda/2$). As

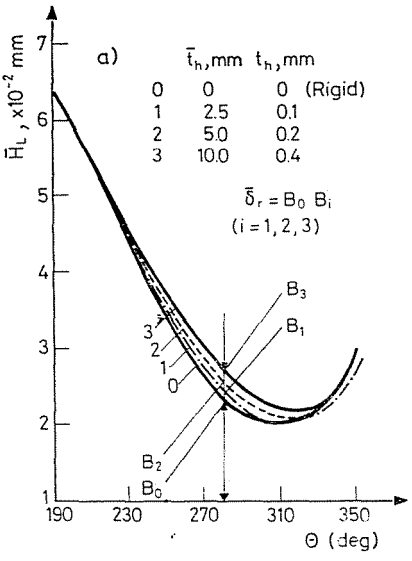

Fig. 2a. Effects of bearing deformation on fluid film thickness

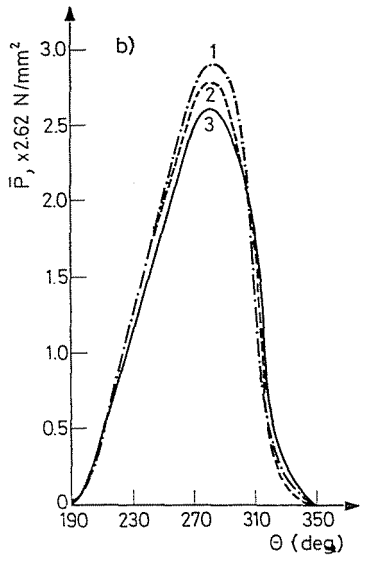

Fig. 2b. Effects of bearing deformation on pressure distribution

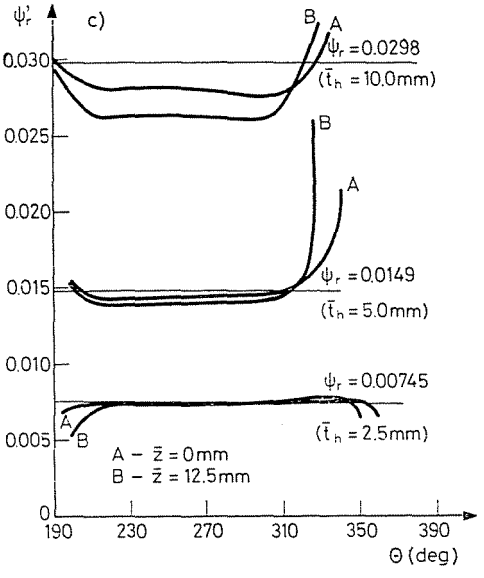

Fig. 2c. Comparison of three-dimensional and plane strain models

may be seen, for a sufficiently large positive pressure zone ψ_r' is nearly constant. This zone of constant ψ_r' widens with decrease in liner thickness thus justifying the use of a linear deformation-pressure relationship given by Eq. (2).

Fig. 2(c) also shows deviation of ψ_r' from ψ_r (as computed from Eq. (3)). As seen from the variation of ψ_r' in the circumferential and axial (from the values at $z=0$, $\pm\lambda/2$) directions, for liner thickness ($\bar{t}_h$) to journal radius ($\bar{R}_j$) ratio less than 0.1, the difference between ψ_r' and ψ_r becomes insignificant. This conclusion is further justified from Table 1 where static characteristics as computed via three dimensional ehd analyses and via simplified linear model are compared for various values of liner thickness.

Table 1

Comparison of static characteristics calculated using 3-d model and plain strain model

$\bar{t}_h$	t_h	Performance	Three dimensional model	Plane strain model	Difference as percent of 3-d values
2.5 mm	0.1	$\bar{p}_{max}$ (N/mm^2)	7.6100	7.616	−0.0686
		$\bar{W}$ (N)	7069.7	7073.1	−0.0463
		$\emptyset$ (deg)	40.84	40.80	+0.0979
5 mm	0.2	$\bar{p}_{max}$ (N/mm^2)	7.2980	7.086	2.897
		$\bar{W}$ (N)	6927.5	6786.9	2.0302
		$\emptyset$ (deg)	39.51	38.62	2.2526
10 mm	0.4	$\bar{p}_{max}$ (N/mm^2)	6.815	6.4780	5.0172
		$\bar{W}_r$ (N)	6660.9	6521.9	2.087
		$\emptyset$ (deg)	37.45	36.04	3.770

With the simplified elastic model, the *ehd* problem of lobed bearing now reduces to finding the solution of Reynolds equation

$$\frac{\partial}{\partial\theta}\left(H_L^3\frac{\partial p_L}{\partial\theta}\right)+\frac{\partial}{\partial z}\left(H_L^3\frac{\partial p_L}{\partial z}\right)=6\frac{\partial H_L}{\partial\theta}+12\frac{\partial H_L}{\partial t} \tag{4}$$

where

$$H_L = e_p-(X_J-X_L)\cos\theta-(Y_J-Y_L)\sin\theta+\psi_r p(\theta, z) \tag{5}$$

is the film thickness in the lobe clearance.

H_L now being a function of pressure, the pressure equation, Eq. (4), of bearing with elastic liner is nonlinear as against the linear equation of the rigid counterpart. The solution, therefore, requires iterations. The finite element method with linear rectangular isoparameteric elements is employed for the solution. Brief details of the solution strategy are given in the next section.

3. Solution scheme

Establishing the steady state pressure field is the prerequisite for computing the static and dynamic characteristics of the bearing. The solution scheme for establishing steady state pressure distribution in the flexible lobed journal bearing is devised by combining sequentially three separately developed programs. These programs are intended to perform individually the following three tasks.

(1) Solving the steady state pressure equation (Eq. (4) with $\partial H_L/\partial t=0$) for each lobe keeping fluid film boundaries fixed. Radial deformation required in the film thickness equation (Eq. (5)) is obtained on the basis of currently available iterations pressures by solving either Eq. (1) or Eq. (2). The iterations are terminated when individual nodal pressure in two successive iterations compare within certain limit.

(2) Establishing the trailing boundary in each lobe satisfying Reynolds boundary condition. The Reynolds boundary is likely to exist if the film terminates before the trailing edge of a lobe. This usually happens in upper lobe. The iterations in determining Reynolds boundary are terminated by putting a limit on pressure induced flow at the boundary which should ideally be zero.

(3) Establishing the journal center equilibrium position for vertical load support. Convergence criterion in this program is applied on the horizontal load component which should ideally be zero.

In the solution of Reynolds equation (program (1)), problem of slow convergence especially at large eccentricities is often encountered. The problem is, however, effectively circumvented if the pressures for the calculation of deformation are taken as some weighted averages of current and previous iteration values rather than the currently available pressures only. Thus the nodal pressures for deformation calculation after j-th iteration are

$$p_i = W_t p_i^j + (1 - W_t) p_i^{j-1}$$

where i is the node number and W_t is weighting factor. Past experience with plain and partial journal bearings [6, 7] has shown W_t equal to 0.6 to be a very suitable choice for wide range of parameters. This value of W_t is found to serve well in the present calculations also.

Expressions for the static characteristics and the calculation method for stiffness and damping coefficients, and hence the stability margins, may be found in relevant literature on lobed bearings [9, 10]. These are not being given here. However, the validity of the devised solution scheme was confirmed by close matching of the calculated performance characteristics of lemon bore bearing with rigid liner ($\psi=0.0$) with those of Lund and Thomeson [10].

4. Results and discussion

The validity of simplified elastic model has been amply justified in Section 2. The performance characteristics of the lemon bore bearings being presented here are computed using this model. The results given in Figs. 3 to 12, are for an aspect ratio $\lambda=1.0$, ellipticity ratios $\varepsilon_p=0.4$ and 0.5, and deformation coefficients $\psi=0.0$, 0.1 and 0.2. The chosen values of λ and ε_p are the commonly used values of these parameters in practical applications. The eccentricity ratios (ε) are taken as high as 0.9 to cover the operating range from a lightly loaded to heavily loaded condition.

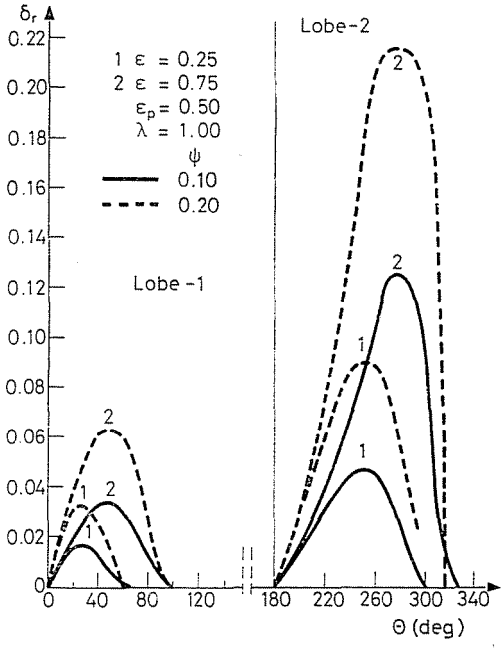

Fig. 3. Radial deformation at bearing mid span ($z=0$)

Fig. 3 presents the plots of liner radial deformation (δ_r), at the centre line of a bearing of ellipticity ratio 0.5 and journal eccentricities 0.25 and 0.75. These curves depict that in both the lobes radial deformation at any point increases with increase in deformation coefficient. The immediate effect of deformation in the liner is obviously found on the pressure distributions in the two lobes. Figs. 4a, b, and c represent the change in pressure profiles (at the center line, $z=0$) with liners deformations ($\psi\neq 0$) from that of its undeformed state ($\psi=0$) at selected eccentricity and ellipticity ratios. Against the increase in positive pressure zone and decrease in maximum pressure with liner deformation as found in circular bearings [6] it is interesting to

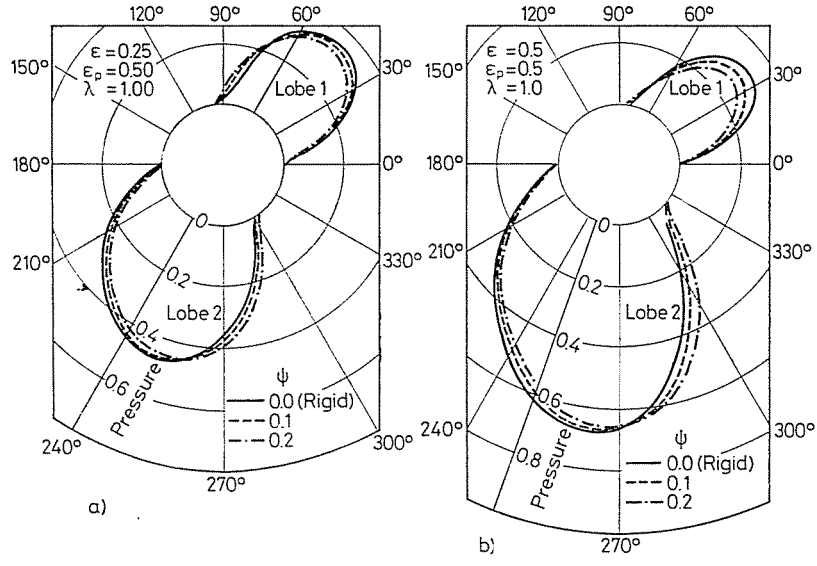

Fig. 4ab. Pressure distribution in flexible two lobe bearing (at $z=0$)

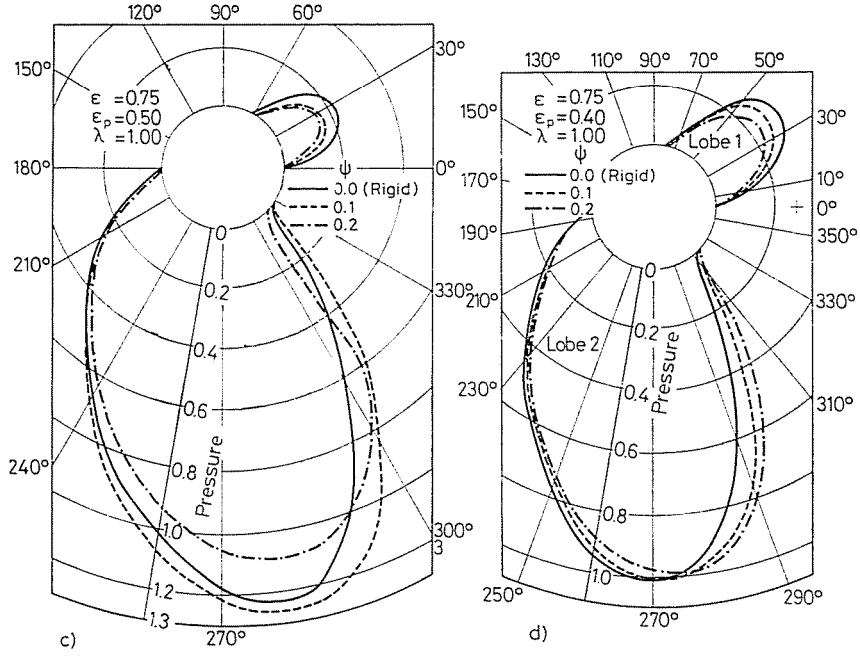

Fig. 4cd. Pressure distribution in flexible two lobe bearing (at $z=0$)

note that in case of lemon shaped bearings this trend may reverse in the bottom lobe at higher eccentricities. Upto moderate eccentricities (<0.7), however the similar changes as in the circular bearing due to liner deformation on pressure distribution are observed, Fig. 4a, 4b. Fig. 5 clearly shows above stated effect of liner deformation on p_{max} of various eccentricities.

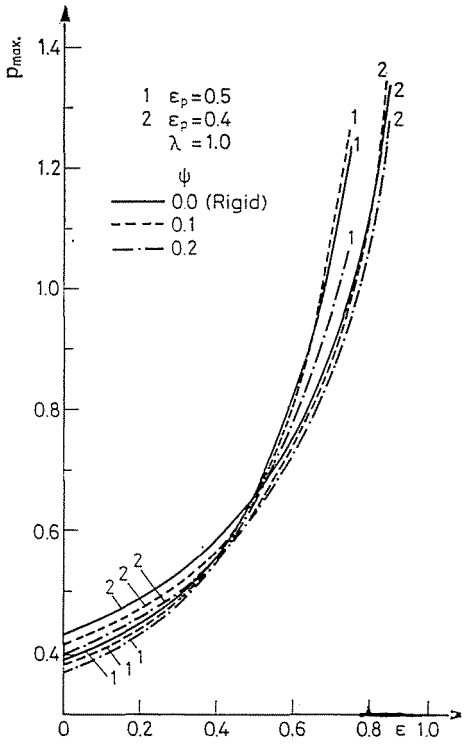

Fig. 5. Maximum pressure vs eccentricity ratio

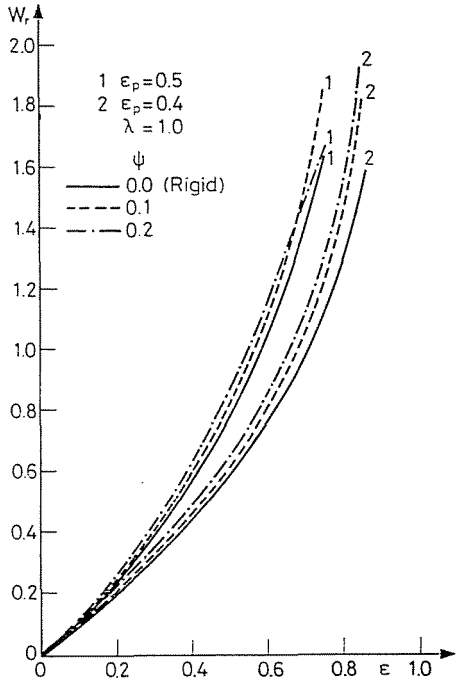

Fig. 6. Load capacity vs eccentricity ratio

Fig. 6 presents the important results related to change in load capacity of lemon shaped bearing with liner deformation. Contrary to decrease in load capacity of the journal bearing system with increase in liner deformation as occurs in circular and partial bearings [6], load capacity of lemon shaped bearing usually increases with liner deformation upto common operating eccentricities (0.75) for both the selected ellipticity ratios (0.4 and 0.5) and deformation coefficients (upto 0.2). It is also seen that the increasing trend of load capacity with increase in deformation coefficient becomes opposite at higher eccentricity (>0.75) in case of the bearing with ellipticity ratio 0.4.

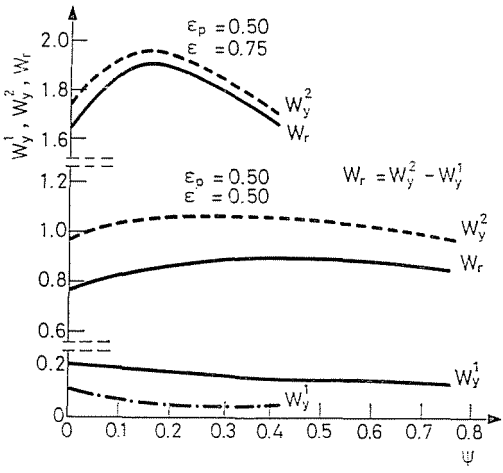

Fig. 7. Lobes contributions in bearing load capacity vs deformation coefficient

The variation of the load capacity with deformation coefficient may be understood more clearly from Fig. 7 which includes the separate contributions of the two lobes. The load component W_y^1 always decreases with increase in deformation coefficient while the component W_y^2 first increases upto a certain value of ψ and then starts decreasing with further increase in ψ. It may now be seen that for a bearing of particular ellipticity and operating eccentricity a deformation coefficient can be selected which would give maximum load capacity. Thus, for instance, for the pair of parameters (ε_p=0.5, ε=0.5) and (ε_p=0.5, ε=0.75) values of ψ for maximum load capacity are 0.175 and 0.45 respectively.

Fig. 8 shows significant change in attitude angle with bearing deformation. At any eccentricity ratio decrease in attitude angle with increase in deformation coefficient in conductive to better stability of the bearing of flexible liner.

Figs. 9 and 10 represent the quantitative effects of deformation coefficient on power loss and lubricant flow for the journal bearing system required to carry certain external load. At any load capacity, appreciable decrease in power loss with increase in deformation coefficient is found. This is an important factor in favour of designing a journal bearing system with flexible liner.

Since bearing deformation modifies the film thickness along the axial length of the bearing and subsequently the pressure gradient, the flow through sides also changes. Depending upon the value of pressure gradient, the lubricant flow is resisted. Fig. 10 is devoted to such effect of bearing liner deformation to lubricant flow.

Fig. 11 presents the critical mass of the journal bearing system with load capacity (W_r). For the selected ellipticity ratios, it is found that upto certain load capacity,

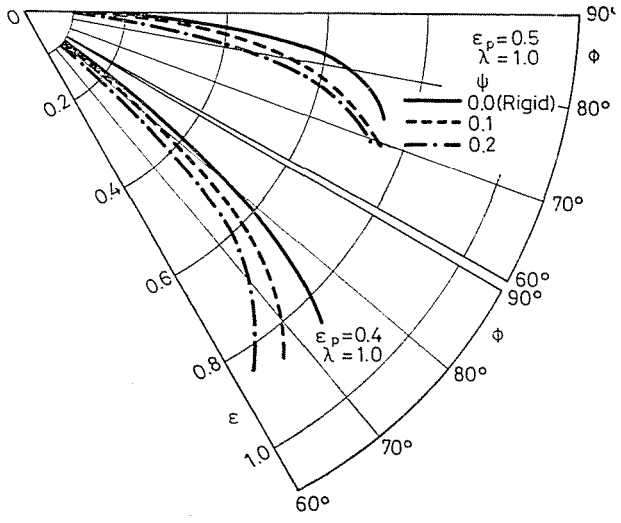

Fig. 8. Attitude angle (Ø) vs eccentricity ratio (ε)

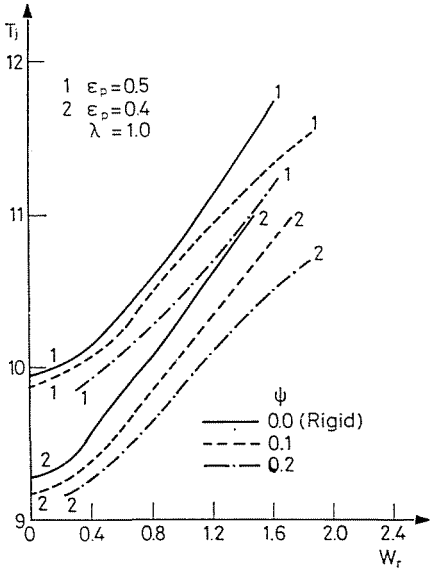

Fig. 9. Frictional torque vs load capacity (W_r)

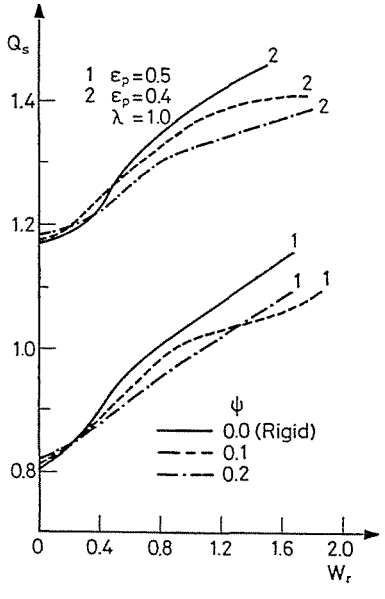

Fig. 10. Side leakage vs load capacity

stability zone remains more for a flexible bearing with certain ψ against that of rigid one. This trend reverses with further increase in load capacity. A comparison of certain load capacity reveals that critical mass first increases with increase in bearing flexibility and then may decline at higher deformation coefficient if load capacity is large. A clear demonstration to this effect is given in Fig. 12. In this figure curves are drawn between M_c and ψ for different eccentricity ratios. At low values of eccentricity ratios (0.1, 0.25, 0.3), increase in M_c is found for large deformation coefficient. At a large eccentricity, however, a value of deformation coefficients accordingly can be obtained to give maximum stability zone.

Based on the analysis and the results presented in nondimensional form in the previous parts, a realistic and easily graspable qualitative comparisons of the dimensional performances of the journal bearing systems with and without deformable liner are presented in Tables 2, 3 and 4. The results in these tables are derived for the following operating parameters:

Table 2

Comparison of rigid and flexible bearing performance characteristics

$\bar{\varepsilon}$ mm	ε	$\bar{l}_h$ mm	ψ	$\bar{\varepsilon}_p = .0195$ mm ($\varepsilon_p = 0.4$)		$\bar{\varepsilon}_p = .0244$ mm ($\varepsilon_p = 0.5$)	
				$\bar{W}_r$ kN	$\emptyset$ deg	$\bar{W}_r$ kN	$\emptyset$ deg
		rigid	0.0	16.57	80.0	21.90	84.00
0.0244 mm	0.5	1.625	0.1	17.13	78.0	23.03	81.00
		3.250	0.2	18.25	75.0	24.15	78.15
		rigid	0.0	21.06	79.5	29.48	82.00
0.0292 mm	0.6	1.625	0.1	22.75	76.0	31.17	77.90
		3.250	0.2	24.15	74.0	32.57	76.20

Table 3

Comparison of rigid and flexible bearing load capacities

$\bar{\varepsilon}$ mm	$\bar{l}_h$ mm	ψ	$\bar{W}_r$ kN		
			$\bar{\varepsilon}_p = .0146$ mm	$\bar{\varepsilon}_p = .0195$ mm	$\bar{\varepsilon}_p = .0244$ mm
	rigid	0.0	19.23	31.17	45.77
0.0365 mm	1.525	0.1	22.04	34.26	51.95
	0.200	0.2	23.87	36.51	51.55

Table 4

Comparison of performance characteristics of rigid and flexible bearings acted upon by uniform load ($\bar{W}_r = 22.5$ kN)

$\bar{t}_h$ mm	$\bar{\varepsilon}_p = .019$ mm ($\varepsilon_p = 0.4$)		$\bar{\varepsilon}_p = .0244$ mm ($\varepsilon_p = 0.5$)	
	ε	$\bar{T}_j$ Nm	ε	$\bar{T}_j$ Nm
rigid	0.58	.7429	0.510	.7821
1.625	0.56	.7274	0.495	.7746
3.250	0.54	.7119	0.475	.7537

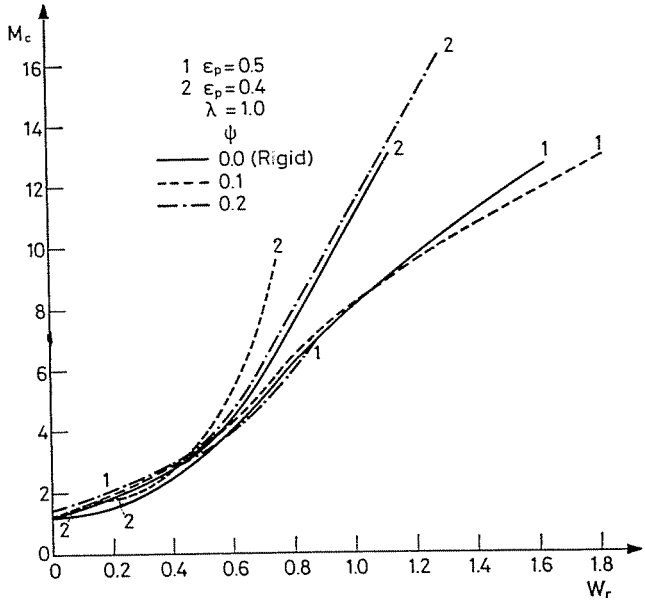

Fig. 11. Critical mass vs load capacity

$\bar{B} = 65$ mm, $\bar{R}_j = 32.5$ mm, $\bar{\mu} = 40$ mPas,
$\bar{\omega}_j = 15\,000$, rpm, $\bar{C}_m/\bar{R}_j = .0015$,
$\bar{E} = 0.98$ MN/m^2 (Young's modulus for brass),
$\bar{t}_h = 1.625$ mm.

These parameters yield the deformation coefficient (ψ) nearly equal to 0.1. A larger value of deformation coefficient approximately equal to 0.2 is obtained with a liner of 3.25 mm thickness.

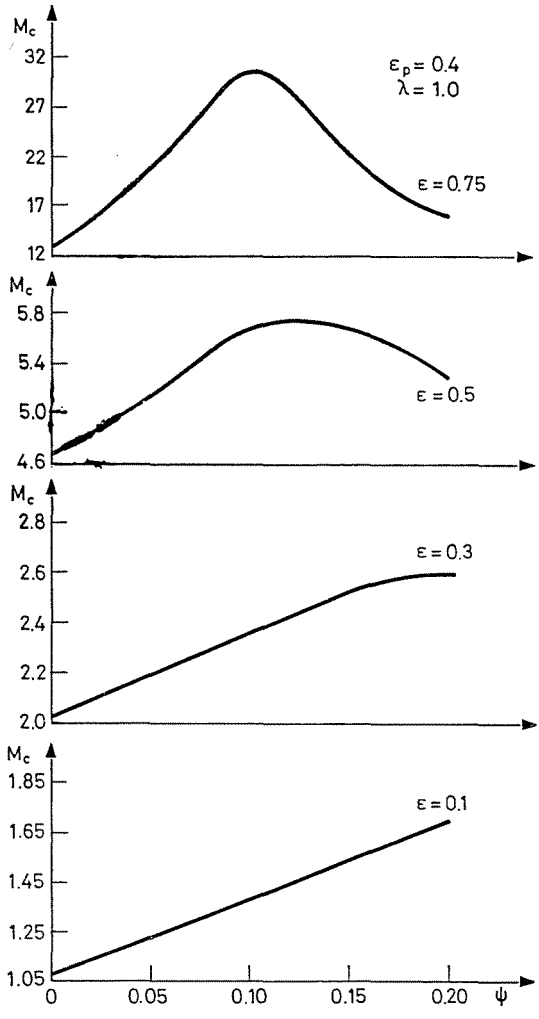

Fig. 12. Critical mass (M_c) vs deformation coefficient (ψ)

Table 2 shows that at the choosen eccentricity ratio 0.6, the attitude angle reduces from 82° to 79.5° if bearing with ellipticity ratio 0.5 is replaced by that of 0.4 when the bearing liner is rigid. More declination in attitude angle is further obtained as low as 74° if instead of rigid lobes ($\psi=0$), lobes with compliant liners of brass ($\psi=0.2$) are used. These results give primary indication that using a bearing with soft liner, better stability at any eccentricity ratio can be attained. Another important result regarding the load capacity shows opposite effects of ellipticity and deformation coefficient. Reduction in load capacity from 29.48 kN to 21.06 kN due to decrease in

ellipticity from 0.5 to 0.4 in case of rigid bearing is partially compensated if rigid liner is replaced by deformable elastic liner. In this example, the load capacity increases from 21.06 kN of rigid case to 24.16 kN when bearing is allowed to deform. Table 3 shows similar observation for the three ellipticities .0146 mm, .0195 mm and .0244 mm and a higher operating eccentricity ($\bar{\varepsilon}$=.0365 mm).

Table 4 presents the difference in the performance of the lemon bore journal bearings with elastic and rigid liners under the condition of same load support ($\overline{W}$)= =22 kN); the other condition like speed, viscosity and bearing geometry being the same as in the previous example. A higher ellipticity bearing runs at larger eccentricity. Moreover, a decrease in eccentricity of any journal bearing system, subjected to some load (22 kN) and of constant ellipticity, can be obtained by using the flexible liner. In the present case for ε_p=0.4, eccentricity reduces from 0.58 to 0.54 as ψ changes from 0.0 to 0.2. Use of flexible liner also reduces the resistance caused by fluid friction in running the shaft. The table shows that frictional torque on the shaft goes down from 0.743 Nm to 0.711 Nm with the change in ψ from 0.0 to 0.2.

5. Conclusions

The results presented in this paper lead to the following conclusions:

(1) For liner thickness to journal radius ratio less than 0.1 deformation in the liner can be determined by a simplified elastic analysis.

(2) For the selected ellipticity ratios, the load capacity at any ε increases upto a certain value of ψ. This increase in load capacity is quite significant. Further increase in ψ results in decrease in load capacity.

(3) With increase in ψ line of centres of the journal and the bearing come closer to load line giving an indication of extended stability zone of the journal bearing system.

(4) A bearing with flexible liner operates with considerably reduced viscous friction torque and side flow from the bearing.

References

1. CARL, T. E., The Experimental Investigation of a Cylindrical Journal Bearing Under Constant and Sinusoidal Loading, Proc. 2nd Convention Lub. and Wear, Instn. of Mech. Engrs, p. 100 (1964).
2. HIGGINSON, C. R., The Theoretical Effects of Elastic Deformation of the Bearing Linear on Journal Bearing Performance, Proc. of Symposium on Elastohydrodynamic Lubrication, Instn. of Mech. Engrs, London, Vol. *180* (3B), p. 31 (1965).

3. O'DONGHUE, J. P., BRIGHTON, D. K., and HOOK, C. J., The Effect of Elastic Distortions on Journal Bearing Performance, Trans. ASME, J. of Lub. Tech., Vol. *89*, p. 409 (1967).
4. CONWAY, H. D. and LEE, H. C., The Analysis of the Lubrication of Flexible Journal Bearing, Trans. ASME J. of Lub. Tech., Vol. *97*, p. 599 (1975).
5. OH, K. P. and HUEBNER, K. H., Solution of the Elastohydrodynamic Finite Bearing Problem, Trans. ASME J. of Lub. Tech., Vol. *95*, p. 342 (1973).
6. JAIN, S. C., SINHASAN, R. and SINGH, D. V., A Study of EHD Lubrication in a Journal Bearing with Piezoviscous Lubricants, ASLE Trans. Vol. *27*, 2, p. 168 (1984).
7. JAIN, S. C., SINHASAN, R. and SINGH, D. V., A Study of Elastohydrodynamic Lubrication of a Centrally Loaded 120° arc Partial Bearing in Different Flow Regimes, Proc. Instn. Mech. Engrs., Vol. *1970*, p. 97 (1983).
8. GATHIN, D. T., An Investigation into Plain Journal Bearing Behaviour Including Thermo Elastic Deformation of the Bush, Proc. Instn. Mech. Engrs., Vol. *199C*, p. 215 (1985).
9. PINKUS, O., Analysis of Elliptical Bearings, Trans. ASME Vol. *78*, pp. 965 (1956).
10. LUND, J. W. and THOMESON, K. K., A Calculation Method and Data for the Dynamic Coefficients of Oil-Lubricated Journal Bearings, Topics in Fluid Film Bearings and Rotor Bearing System Design and Optimization, The ASME Design Conf., pp. 1—29 (1978).

S. C. JAIN
M. MALIK
R. SINHASAN
Roorkee, 247 667, India